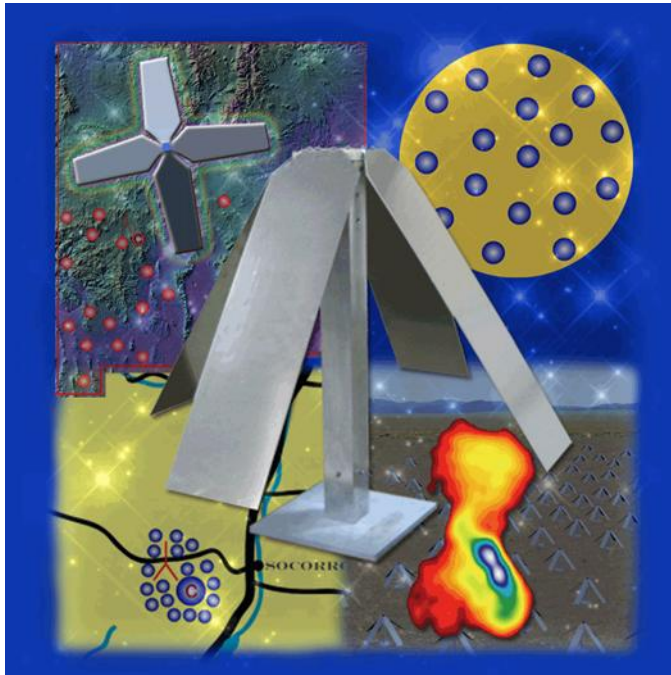


CEDAR-2012

Mesoscale Ionospheric Sensing Using Modern Radio Interferometers



Dr. Kenneth F. Dymond
Space Science Division
Naval Research Laboratory
Washington, DC

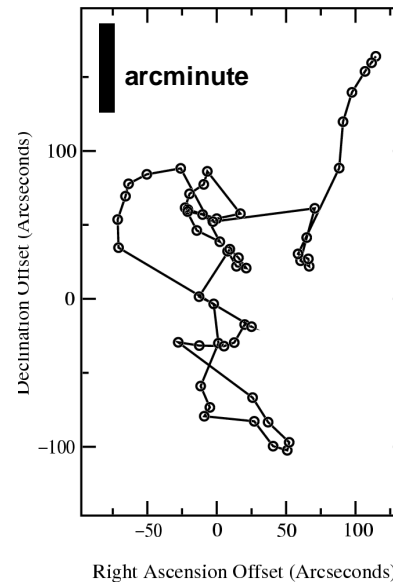
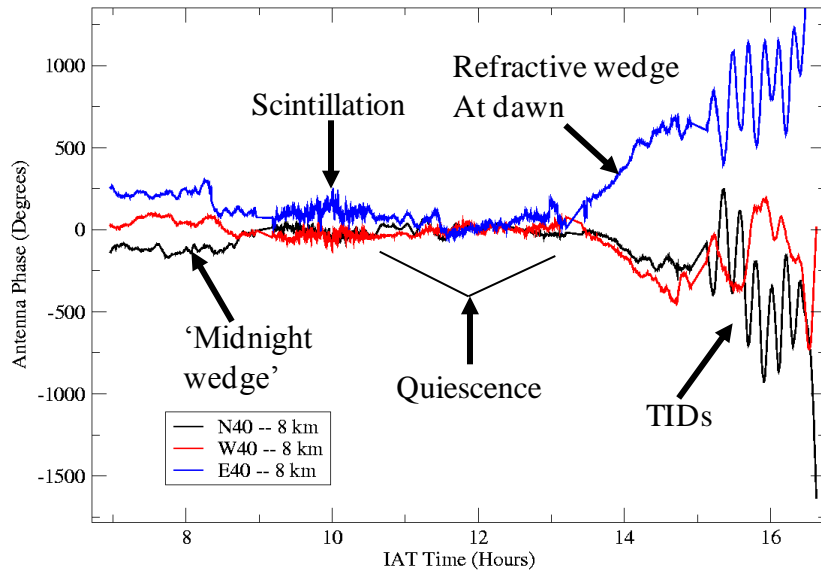
Overview

- Several next-generation astronomical radio interferometers are either operating or under construction
 - *Two northern hemisphere (EVLA/LWA, New Mexico, USA; LOFAR, Northern Europe primarily Netherlands)*
 - *Two proposed in the southern hemisphere (SKA, South Africa or Australia; MWA Australia)*
 - *Two equatorial (GMRT, India; ALMA, Chile)*
- Ionospheric effects including refraction, diffraction, scintillation, and Faraday rotation can affect astrophysical measurement quality
 - *Better ionospheric correction methods are needed to improve astrophysical imaging*
 - *However, the astrophysical observations can be exploited to better understand mesoscale ionospheric effects*
- Modern radio interferometers present new opportunities for ionospheric science



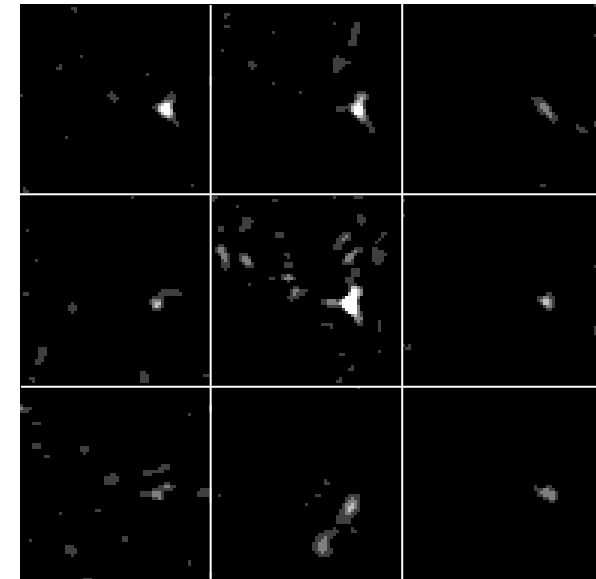
Ionospheric Effects on LF Astronomical Imaging

- Ionospheric effects are very important
 - *Correction is required to meet imaging goals*
 - *Ionospheric specification/measurement is a byproduct of ionospheric correction/calibration*



1 minute sampling intervals

9 sources showing refractive wander



6/28/2012

3

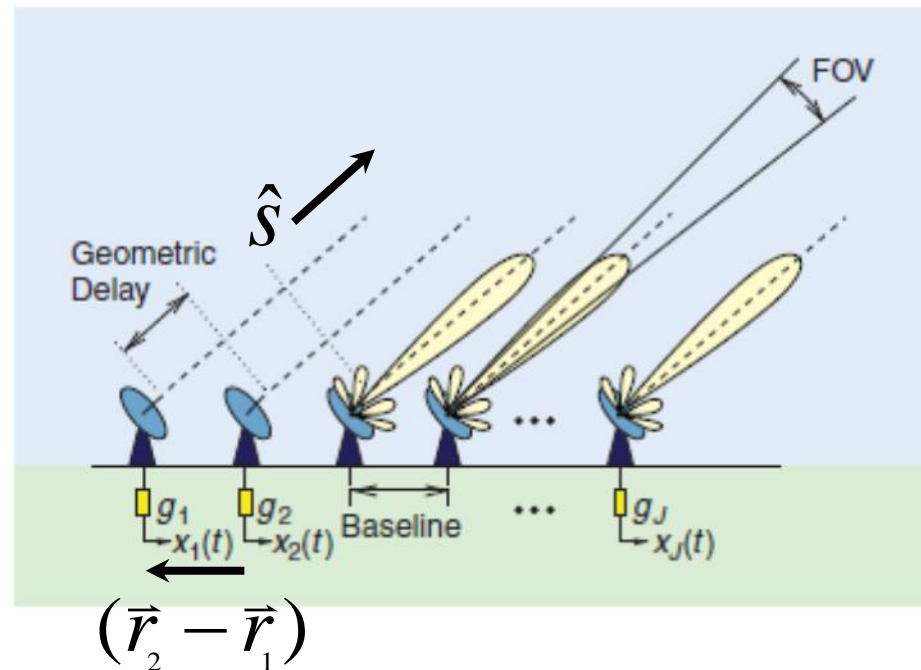


How Do Interferometers Work?

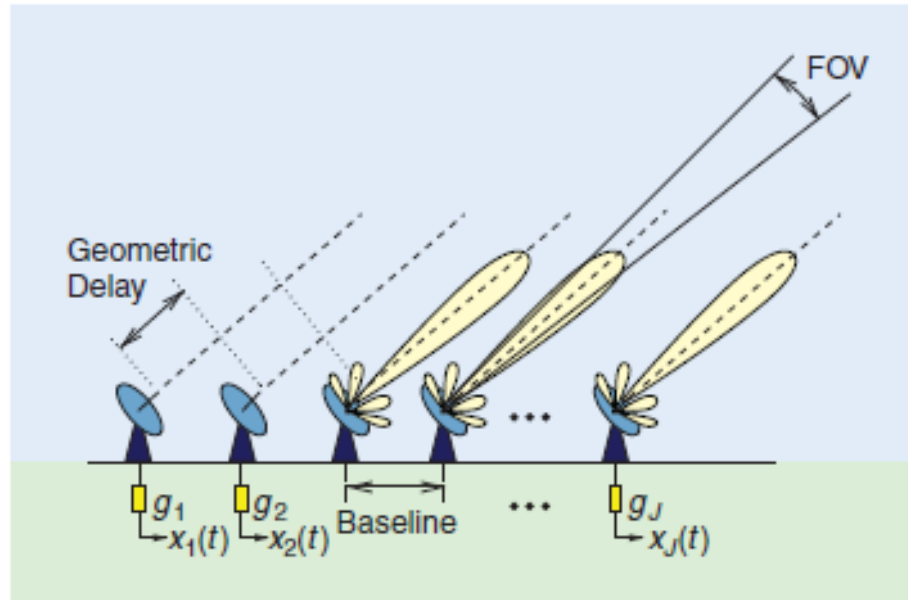
- Interferometers measure the quasi-monochromatic fringe visibility V
- V is the interferogram of sources visible within the beam of the interferometer
- The Visibilities and the Brightness (B) are a Fourier transform pair
- The Brightness is seen to be only a function of the baseline distance between the antennas
- The slow rotation of the Earth causes the dot product to vary with time effectively scaling the baseline distance
- This improves the coverage in the spatial frequency domain and improves the retrieved image quality

$$V_{\nu}(\bar{r}_1, \bar{r}_2) = \int B_{\nu}(\hat{s}) \exp -2\pi i \hat{s} \cdot (\bar{r}_2 - \bar{r}_1) / \lambda \, d\Omega$$

$$B_{\nu}(\hat{s}) = \int V_{\nu}(\bar{r}_1, \bar{r}_2) \exp 2\pi i \hat{s} \cdot (\bar{r}_2 - \bar{r}_1) / \lambda \, d\Omega'$$



Measurement Imperfections (1 of 2)



- But the interferometers are imperfect and instrumental and other artifacts creep into the measurements
- *Geometric and antenna delays*
 - *Point spread function of antennas*
 - *Assumption that celestial sphere does not affect transmission of radio waves – ionospheric distortions violate this assumption*



6/28/2012

5



Measurement Imperfections (2 of 2)

- These imperfections affect the measurement equation

$$V_{\nu}^M(\bar{r}_1, \bar{r}_2) = \int B_{\nu}(\hat{s}) g_1 g_2^* \exp[-2\pi i \hat{s} \cdot (\bar{r}_2 - \bar{r}_1) / \lambda] d\Omega$$

- The antenna gain terms (g_1) are given by:

$$g_1 = P_{\nu} \hat{s} \exp(i(\phi_{Amb} + \phi_{Iono} + \phi_{Geom} + \phi_{Ant}))$$

- P_s is the antenna point spread function
 - $\phi_{Amb} = 2\pi$ ambiguities
 - $\phi_{Iono} =$ ionospheric induced phase delay
 - $\phi_{Geom} =$ geometrically induced phase term (Earth's rotation)
 - $\phi_{Ant} =$ phase delay induced by antenna electronics
- The ionospheric terms are what we are interested in
 - The Visibilities are affected by the phase differences:
 - $\Delta\phi = (-8.48 / \nu_{GHz}) \Delta T_{TECU} \sim 0.0015 \text{ TECU deg}^{-1}$ (at 74 MHz)

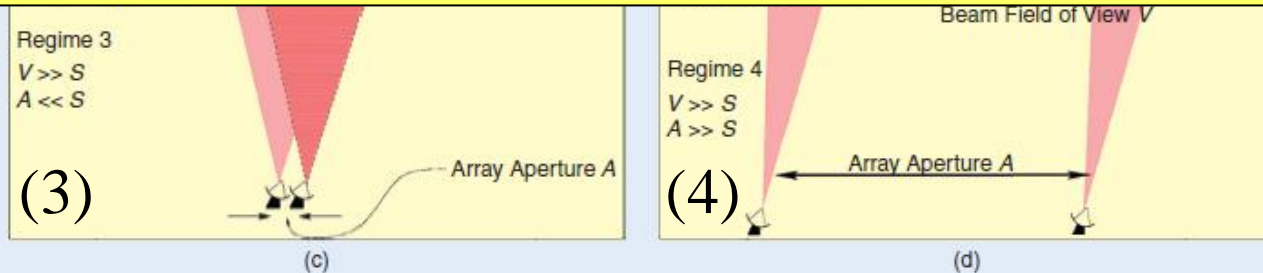


Ionospheric Distortion Scenarios

In scenario 3, the correction is done in image space after the Visibilities are Fourier transformed. A phase screen is fit to minimize image distortions and applied to the Visibilities which are transformed a second time. This is

In scenario 4, it is likely that a hybrid approach will be adopted.

In scenarios 1 & 2, the ionospheric term can be estimated in the spatial frequency space and removed before Fourier transforming. This is known as Self Calibration.



Where Do We Go From Here?

- Self Calibration: works for narrow fields of view and bright sources
- Field Calibration: works well for wider fields of view and for cases when the ionospheric coverage exceeds the array size
- Hybrid Calibration: a combination of self calibration and field calibration
 - *Peeling: Self calibrate on bright sources and then apply field calibration to remove the remaining distortion*
- Can we use ionospheric knowledge to produce a better approach?
 - *Data assimilation: Assimilate heterogeneous ionospheric measurements to create global/regional ionospheric specification*
 - *Phenomenological approach: identify ionospheric phenomena present in data and tailor correction*
- What phenomena are observable?

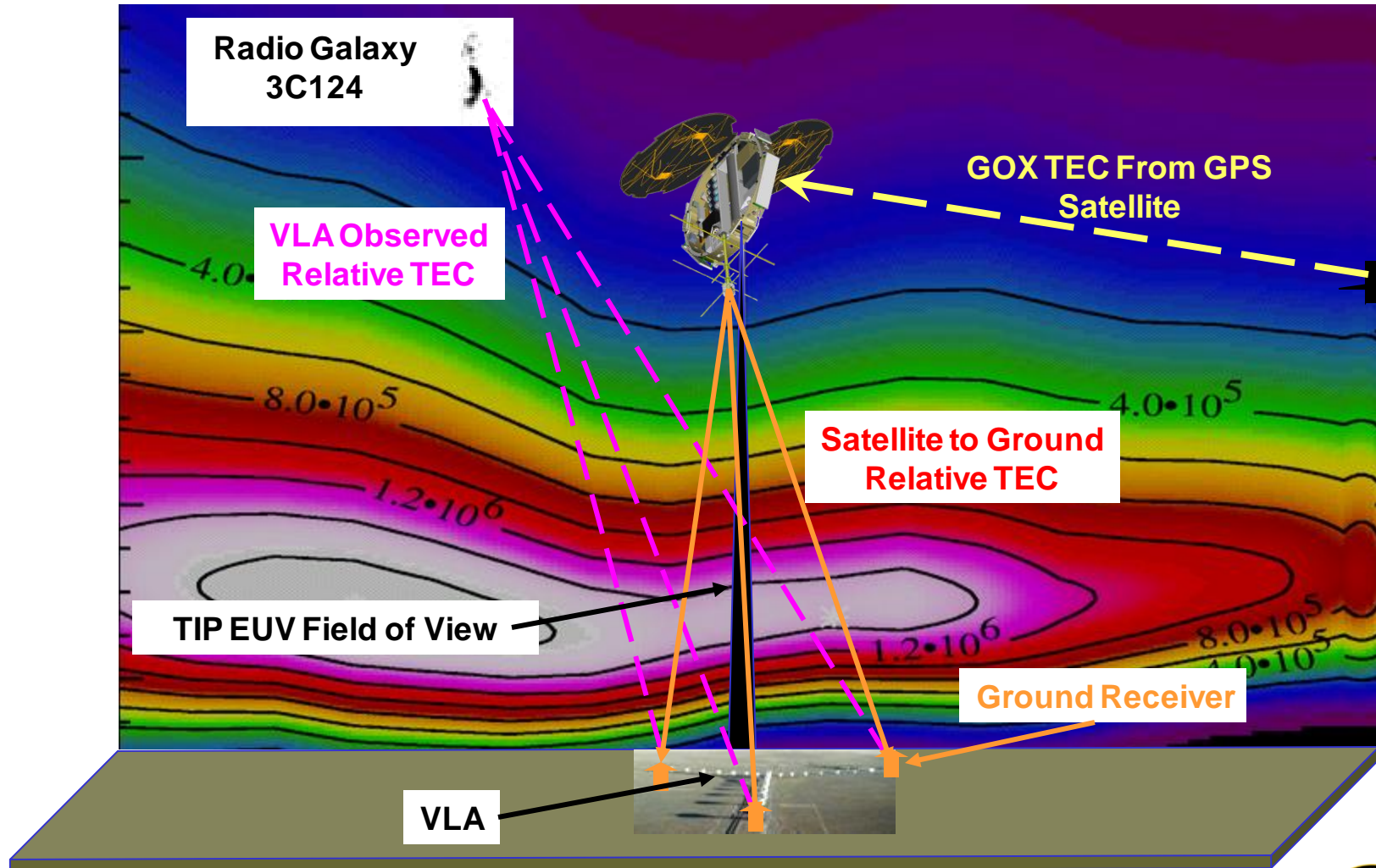


6/28/2012

8



CRICKET Concept



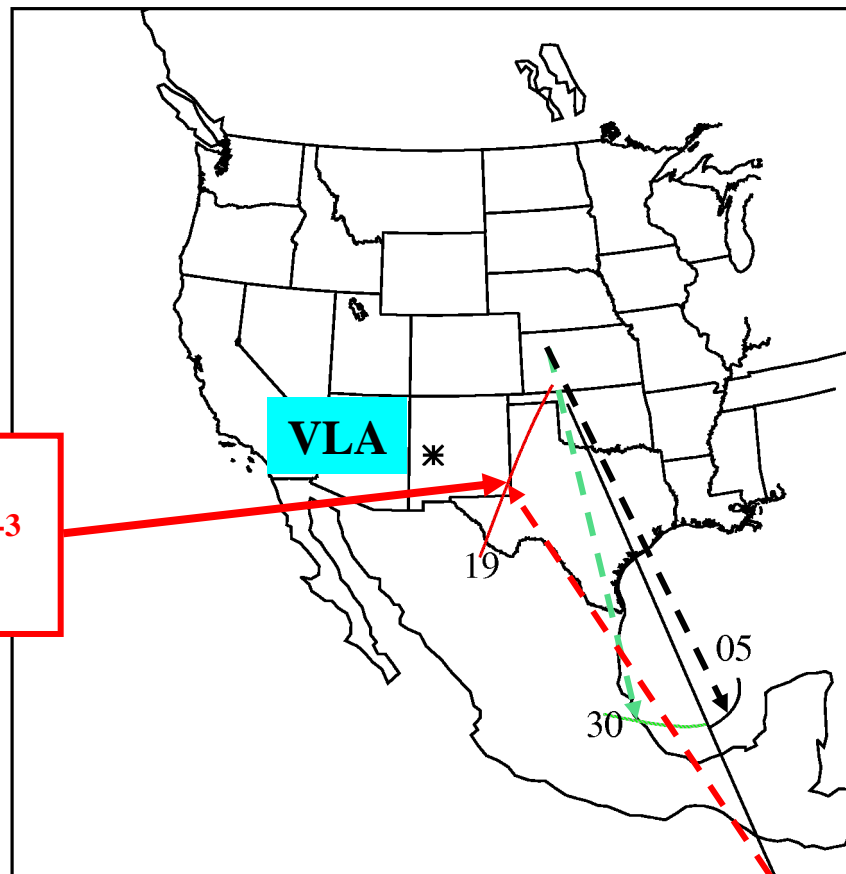
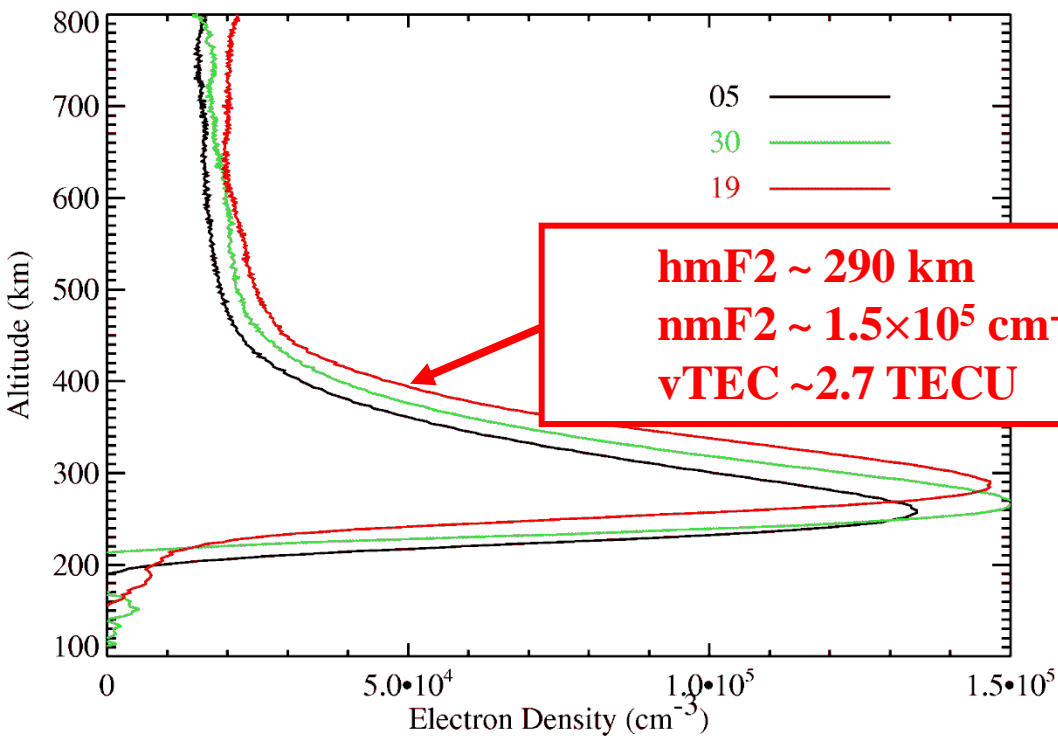
6/28/2012

9



COSMIC-GOX: Electron Density Profiles

- Electron density profiles from three widely separated occultations indicated low gradients in the background ionosphere

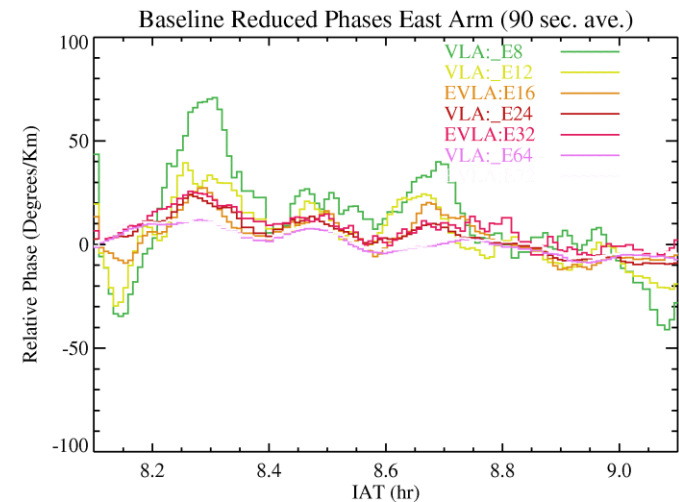
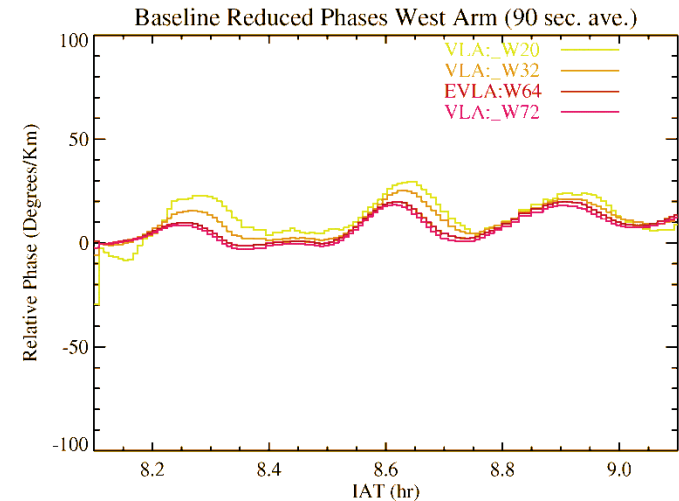
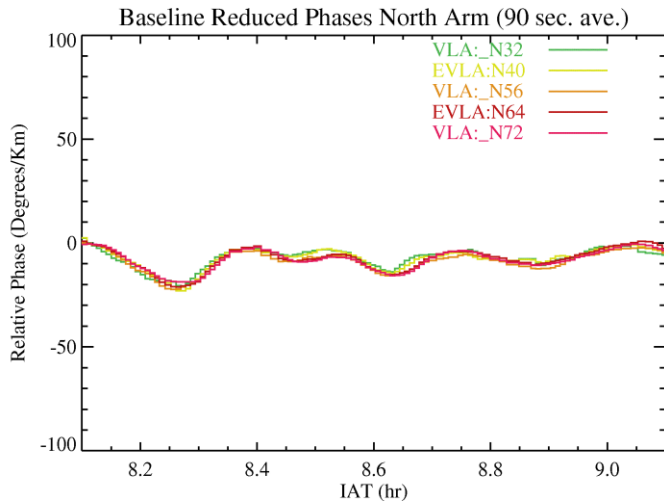


6/28/2012

10



VLA Measurements



- The phases divided by the baseline length are shown
- West & North
 - Phase/TEC gradients approximately proportional to the baseline length implying structures larger than the array dimensions
 - Phase structures along each arm are very similar
 - Phase progression indicating roughly North-to-South motion
- East arm baseline scaling not as clear
- Taken together this indicates a large-scale wave traveling approximately perpendicular to the East arm (moving South-Southwest)



6/28/2012

11



CRICKET Derived TID Parameters

Period (min.)	Amplitude (TECU)	λ (km)	Azimuth (degrees)	Speed (m/s)	Projected λ (km)
95.33	0.010	91.2	186	16	100.7

➤ Results are fairly typical for characteristics of MSTIDs seen over SW US

- *Speeds typically ~100-200 m/s*
- *Wavelengths typically 100-200 km*
- *Periods 10-100 min.*
- *Direction of propagation typically southwesterly – but not always*

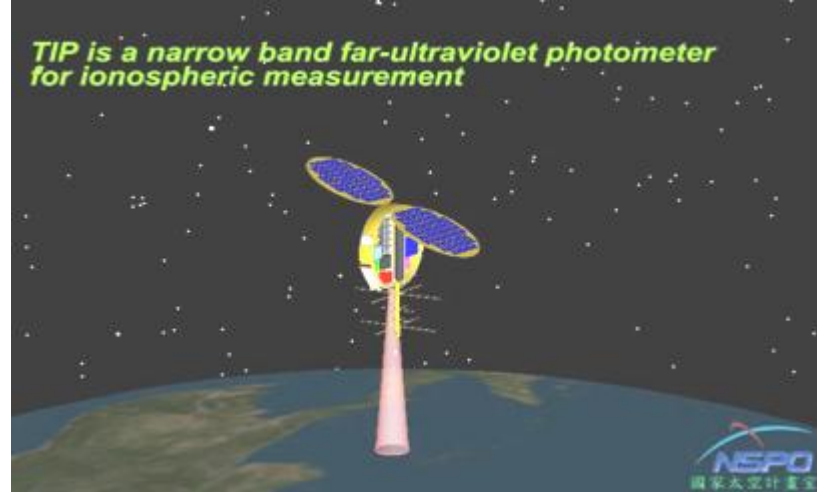
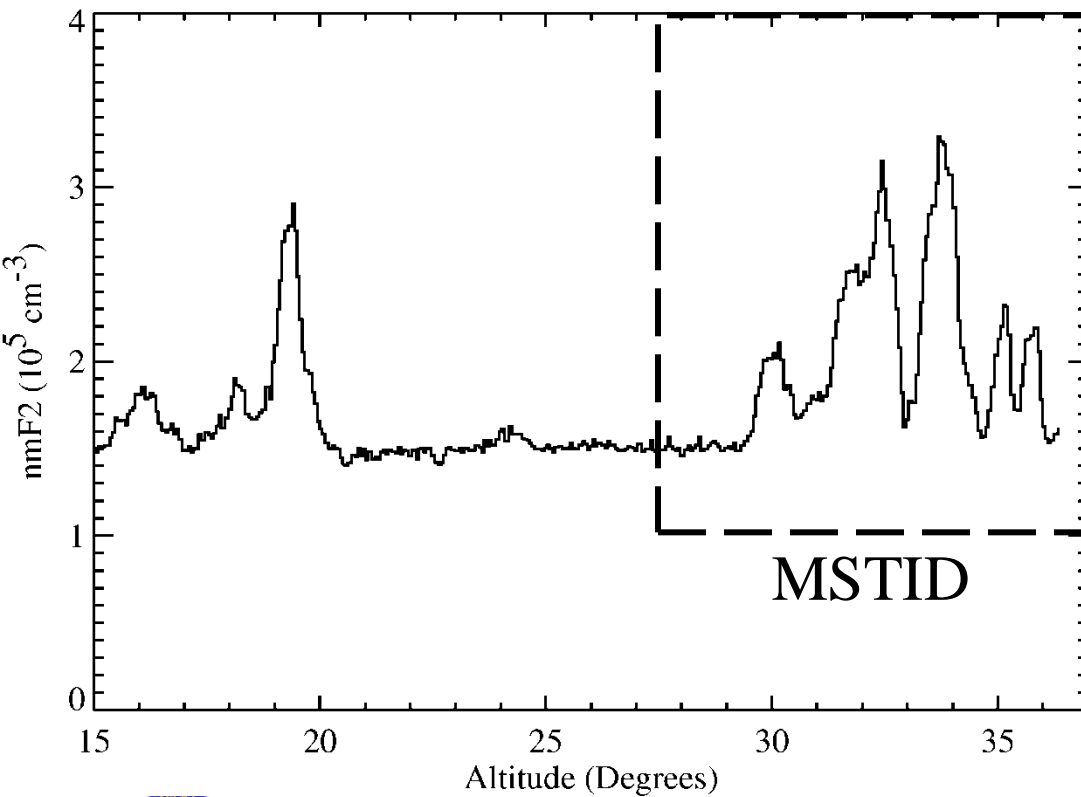
13.62	0.065	78.7	223	96	165.3
11.92	0.141	178.6	121	250	233.4
10.59	0.137	196.1	159	309	196.2

TID



TIP Measurements

➤ TIP measures the UV radiance at 135.6 nm



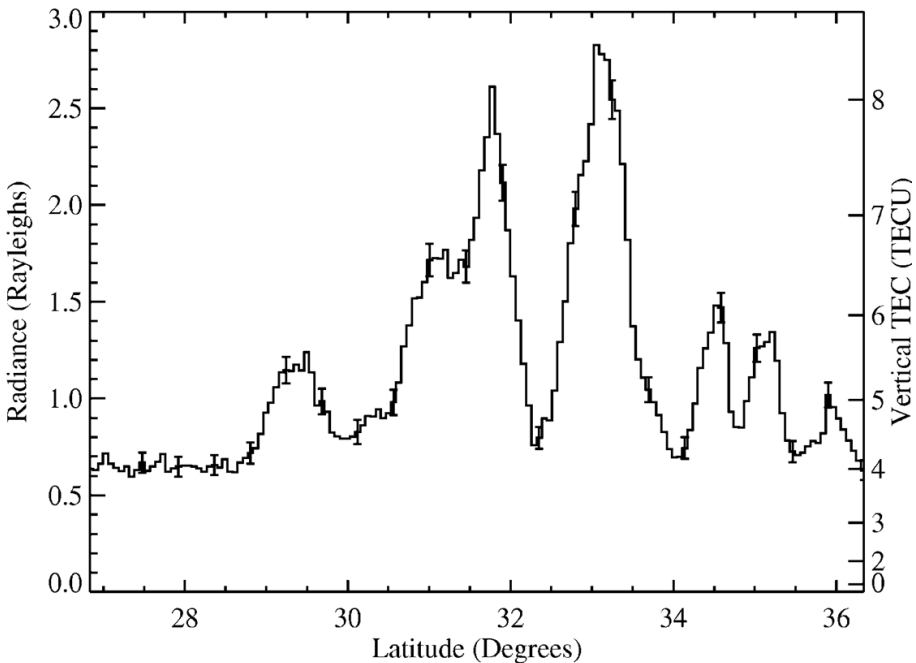
6/28/2012

13

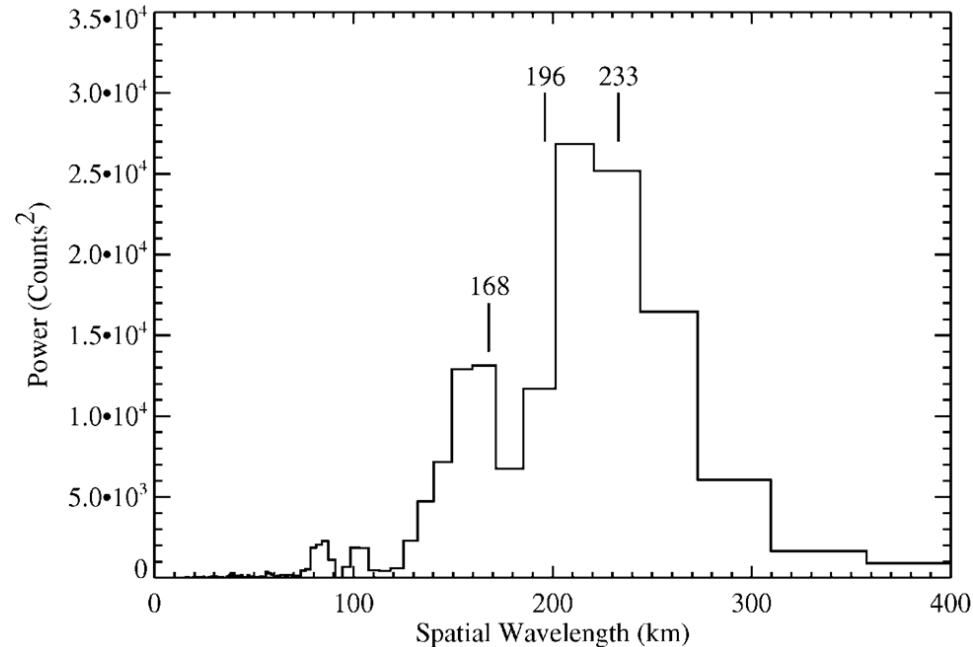


TIP Measurements

TIP Radiance & TEC



Fourier Transform of TIP Data



Three wavelengths seen in TIP data consistent with VLA measurements.



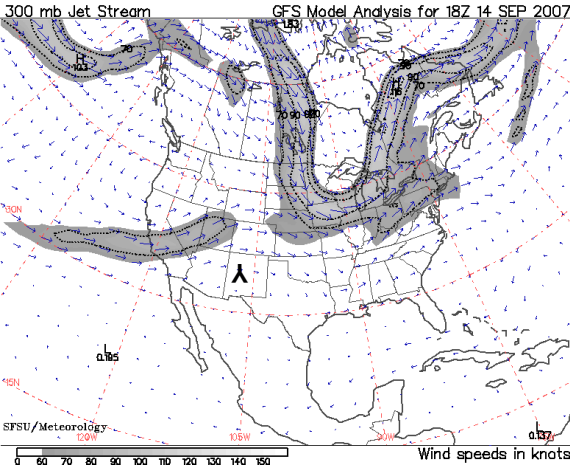
6/28/2012



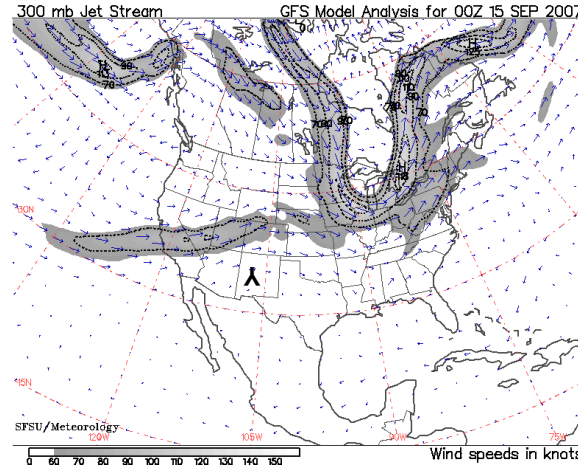
Where did it/they come from?

- Some MSTIDs are thought to originate from turbulence near jet streams
- The jet stream over the central US was changing dramatically on Sept 15, 2007
- This is a possible explanation for their origin

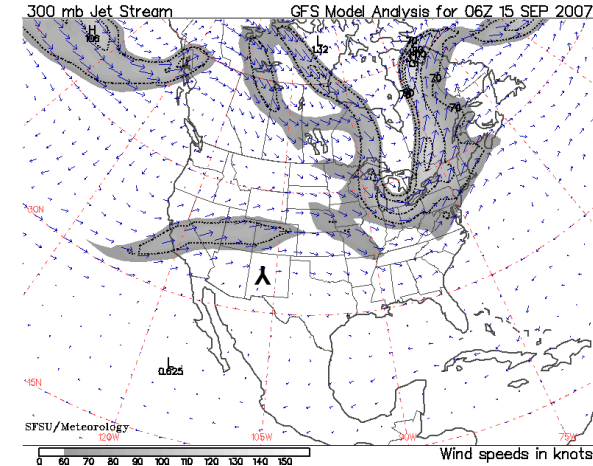
14 Sept, 18 UT



15 Sept, 0 UT



15 Sept, 6 UT

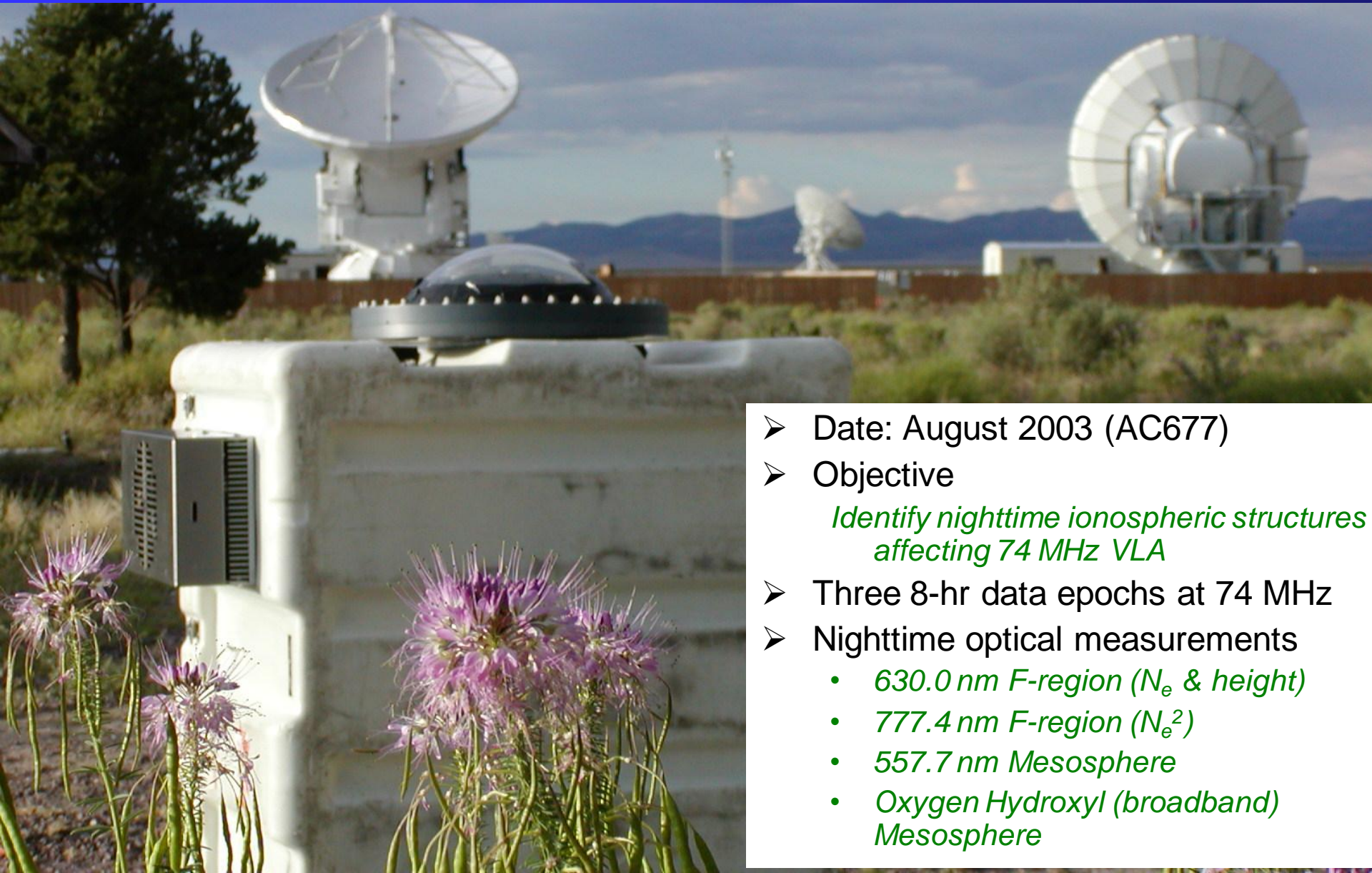


6/28/2012



15

Simultaneous Radio and Optical Observations (Campaign 1)



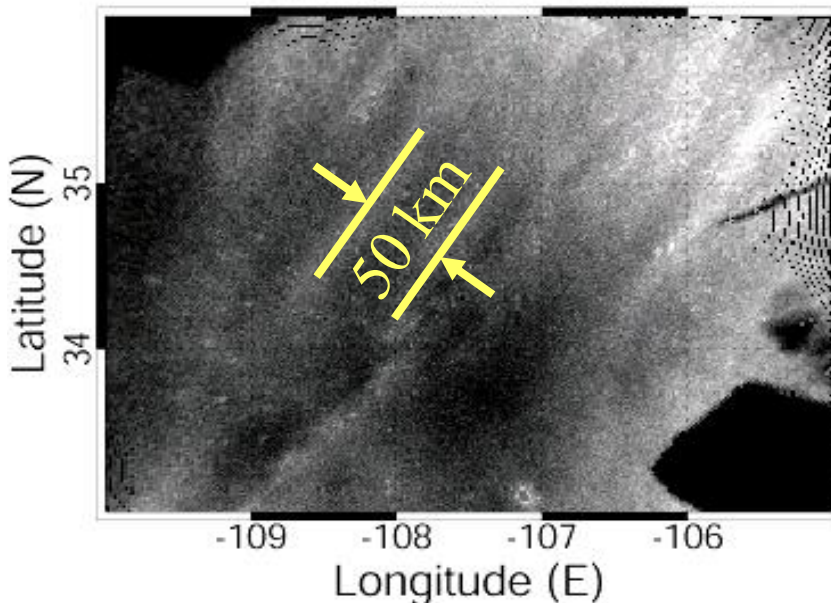
- Date: August 2003 (AC677)
- Objective
 - Identify nighttime ionospheric structures affecting 74 MHz VLA*
- Three 8-hr data epochs at 74 MHz
- Nighttime optical measurements
 - *630.0 nm F-region (N_e & height)*
 - *777.4 nm F-region (N_e^2)*
 - *557.7 nm Mesosphere*
 - *Oxygen Hydroxyl (broadband) Mesosphere*

Mesospheric Waves

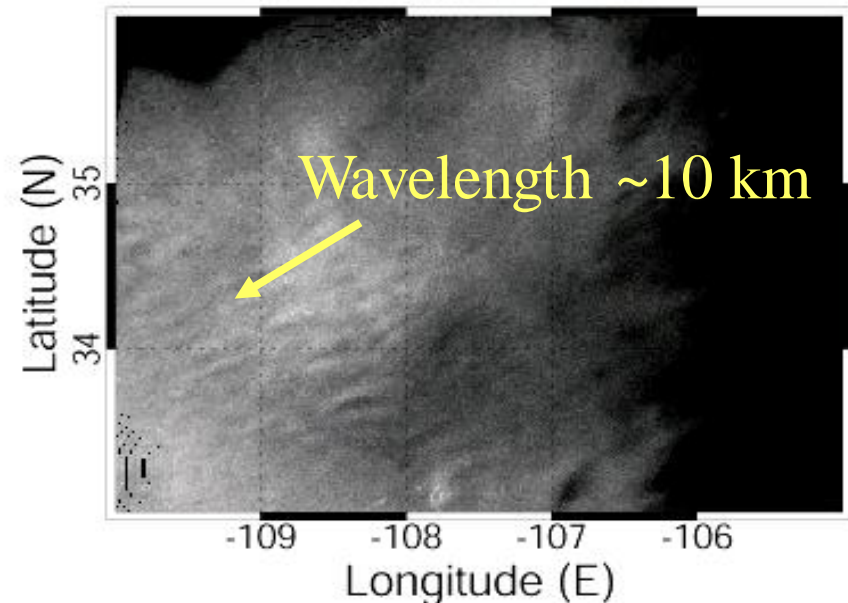
- Complex mesospheric waves observed by optical camera
- Mesosphere – neutral atmosphere, 50–85 km altitude
- Turbulence driven by atmospheric gravity waves

Turbulence suggests the possible existence of Sporadic-E plasma clouds near 100 km altitude

557.7-nm emission
Aug 25, 2003 00:29 UT

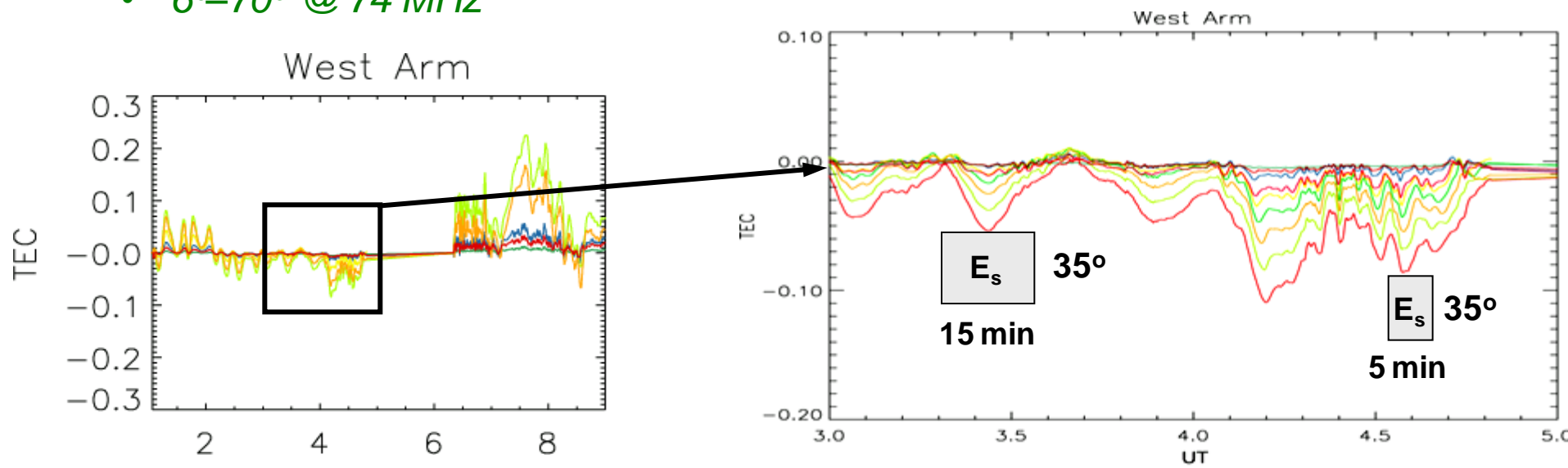
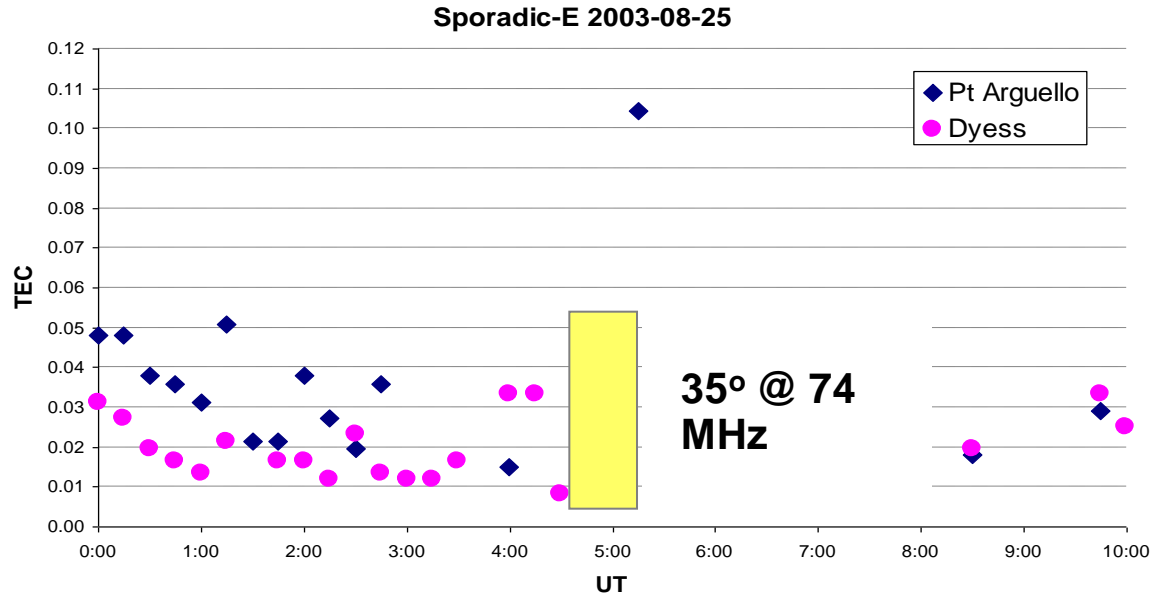


557.7-nm emission
Aug 25, 2003 02:09 UT



Sporadic-E Observations

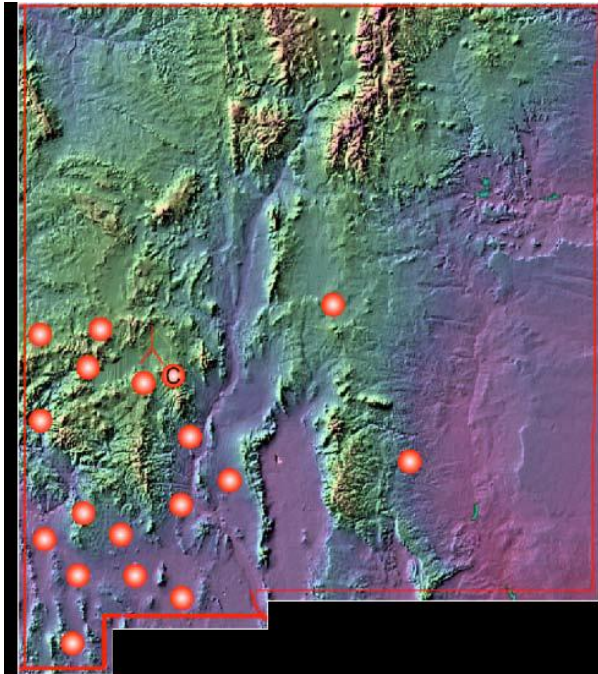
- Top panel: Off-site Ionosonde observations of sporadic-E
- Estimated VLA Es scale sizes match fluctuations in August 2003 VLA data
 - *50 km horizontal scale*
 - *50–150 m/s speed*
 - *5–15 min fluctuations*
 - *6°–70° @ 74 MHz*



LWA Overview

- 52 Stations spread over New Mexico (bottom panel)
- Each station consists of sets of phased array antennas
 - Operates from 20-88 MHz
 - Computer controlled beam steering
- Upper Panel at right LWA station 1
- Lower left panel shows antennas at LWA 1
- First station: 256 antennas, 2.8° Beam width at 75 MHz

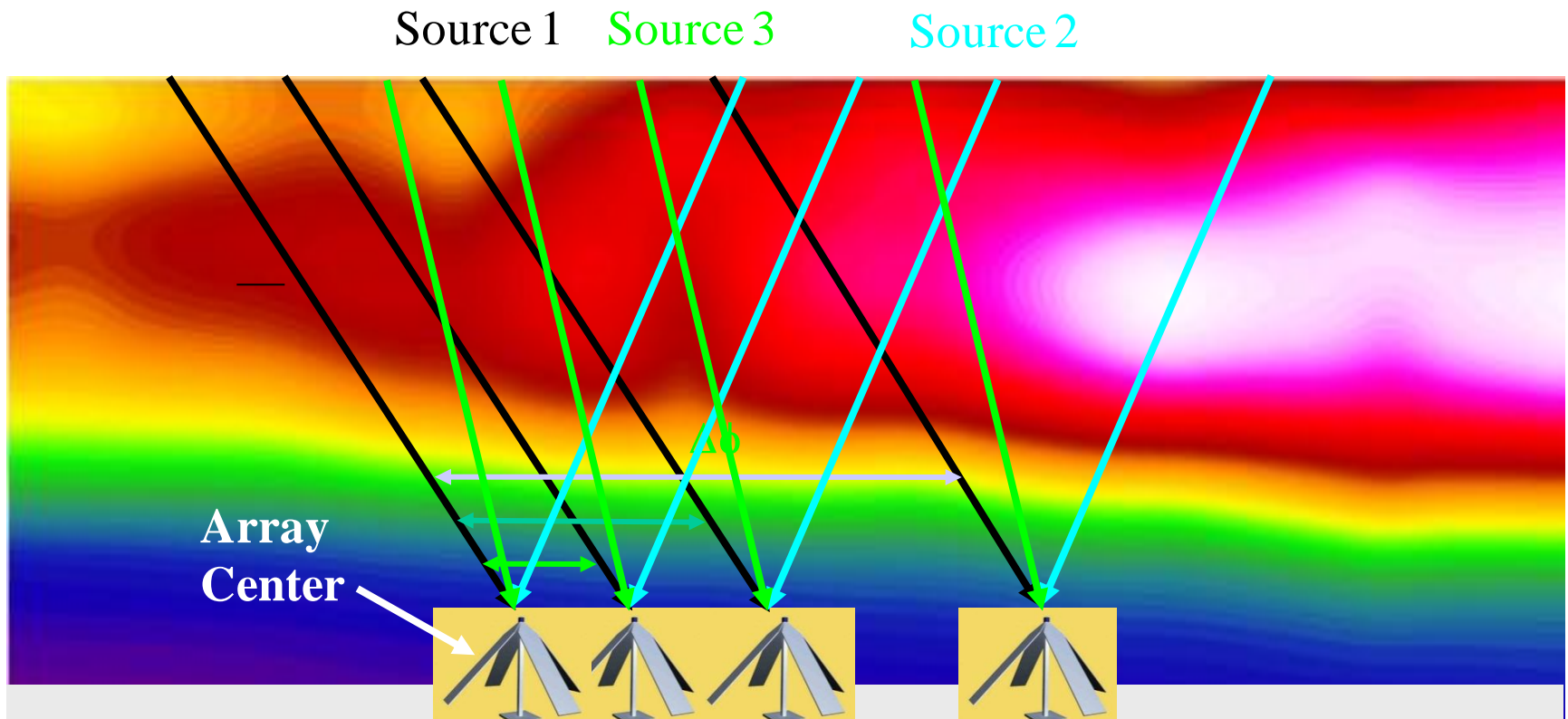
LWA Layout



LWA Station 1 Layout



RASCAL Concept



Rapid All-Sky CALibration (RASCAL) technique proposed to perform ionospheric measurements & calibration

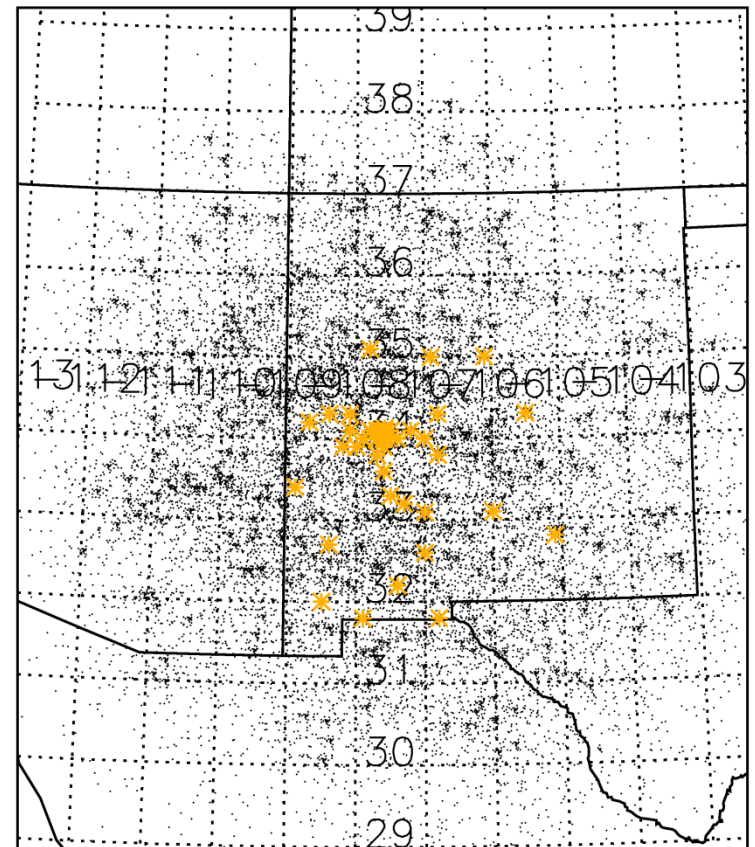
Uses the VLSS sky survey for source selection

RASCAL technique will scan all visible sources with ~ 10 second cadence

Current implementation: ~ 100 sources, 1 station, 50 msec dwell, $\sim 6-7$ sec scan

RASCAL Simulation

- VLSS sky catalog contains:
 - 16612 sources
 - Flux > 1 Jy
- Midnight local time on 3/21/2010
 - 52 LWA stations (yellow stars)
 - Minimum source elevation 30°
 - 339 sources visible with fluxes > 10 Jy
 - Given current operating constraints –
50 ms dwell and 20% switching overhead – ~20 sec required to sample sources
 - For 17628 total lines-of-sight!
 - High sampling density
 - Ionospheric height 300 km



6/28/2012

21



Summary & Conclusions

- Modern array interferometers are extremely sensitive to the ionosphere
 - *Measure the TEC difference between array elements to extremely high precision*
 - *However, they are insensitive to the absolute TEC*
- High temporal resolution ~10 seconds
 - *Good for studying traveling structures: TIDs, Sporadic-E, Ionospheric Gradient Evolution...*
- High spatial resolution ~10 km
 - *Good for mesoscale ionospheric studies*
- New ionospheric correction techniques are required providing opportunities for young researchers
- Also, new measurement and calibration techniques promise new ionospheric measurement types



References

- Wijnholds, S. J., S. van der Tol, R. Nijboer, and A.-J. van der Veen, “Calibration Challenges for Future Radio Telescopes: An overview of a daunting parameter-estimation task”, *IEEE Signal Processing Magazine*, 2010.
- Clark, B. G., “Coherence in Radio Astronomy”, *Synthesis Imaging in Radio Astronomy II*, ASP Conference Series, Vol. 180, 1999.
- Cornwell, T. and E. B. Fomalont, *Self-Calibration, Synthesis Imaging in Radio Astronomy II*, ASP Conference Series, Vol. 180, 1999.
- Dymond, K. F., C. Watts, C. Coker, S. A. Budzien, P. A. Bernhardt, N. Kassim, P. Ray, T. J. Lazio, K. Weiler, P. C. Crane, P. S. Ray, A. Cohen, T. Clarke, L. J. Rickard, G. B. Taylor, F. Schinzel, Y. Pihlstrom, M. Kuniyoshi, S. Close, P. Colestock, S. Myers, and A. Datta (2011), “A Medium-Scale Traveling Ionospheric Disturbance Observed from the Ground and from Space”, *Radio Sci.*, 46, RS5010, doi:10.1029/2010RS004535.
- Coker, C., S. E. Thonnard, K. F. Dymond, T. J. W. Lazio, J. J. Makela, and P. J. Loughmiller (2009), “Simultaneous radio interferometer and optical observations of ionospheric structure at the Very Large Array”, *Radio Sci.*, 44, RS0A11, doi:10.1029/2008RS004079.



Backup Slides



6/28/2012

24



Interferometer Measurements (1 of 2)

- Maxwell's Equations tell us that:

$$\vec{E}(\vec{r}) = \iiint P_v(\vec{R}, \vec{r}) \vec{E}(\vec{R}) dx dy dz$$

- Assume that the celestial sphere is empty

$$\vec{E}(\vec{r}) = \iint \vec{\mathcal{E}}(\vec{R}) \frac{\exp 2\pi i \nu |R - r|/c}{|R - r|} dS$$

- Actually we are interested in the fringe visibility, which is proportional to the expectation value of square of the electric field

$$V_{\nu, \vec{r}_1, \vec{r}_2} = \left\langle \iint \mathcal{E}_\nu(R_1) \mathcal{E}_\nu^*(R_2) \frac{\exp 2\pi i \nu |R_1 - r_1|/c}{|R_1 - r_1|} \frac{\exp -2\pi i \nu |R_2 - r_2|/c}{|R_2 - r_2|} dS_1 dS_2 \right\rangle$$



Interferometer Measurements (2 of 2)

- The source is assumed to emit incoherently, so the integral is zero except when $R_1 = R_2$ and the order of the integrations can be reversed:

$$V_{\nu}(\vec{r}_1, \vec{r}_2) = \iint \langle |\mathcal{E}_{\nu}(R)|^2 \rangle |R|^2 \frac{\exp 2\pi i \nu |R - r_1|/c}{|R - r_1|} \frac{\exp -2\pi i \nu |R - r_2|/c}{|R - r_2|} dS$$

- Assuming that $R \gg r$, expanding the exponentials retaining first order terms, and substituting:

$$I_{\nu}(\hat{s}) = \langle |\mathcal{E}'_{\nu}(\hat{s})|^2 \rangle |R|^2$$

- We get finally the Measurement Equation (\hat{s} is a unit vector pointing toward the source):

$$V_{\nu}(\vec{r}_1, \vec{r}_2) = \int I_{\nu}(\hat{s}) \exp -2\pi i \nu \hat{s} \cdot (\vec{r}_2 - \vec{r}_1)/c d\Omega$$



Total Electron Content Sensitivity (1 of 2)

- For a plane parallel ionosphere:

$$\begin{aligned}\Delta T_{2,1} &= T_2(\vec{r}_2, \hat{s}_2) - T(\vec{r}_1, \hat{s}_1) \\ &= \int_0^{\infty} n(x_2, y_2, z_2) \frac{dz_2}{\mu_2} - \int_0^{\infty} n(x_1, y_1, z_1) \frac{dz_1}{\mu_1}\end{aligned}$$

- Assuming a small spatial extent for the array and expanding in a Taylor series:

$$\Delta T_{2,1} \approx \int_0^{\infty} \left[n(x_1, y_1, z) \mu_1 + \mu_1 \vec{\nabla}_{x,y} n(x_1, y_1, z) \cdot (\vec{r}_2 - \vec{r}_1) - n(x_1, y_1, z) \mu_2 \right] \frac{dz}{\mu_2 \mu_1}$$

- In a plane parallel atmosphere: $\mu_1 = \mu_2$

$$\Delta T_{2,1} \approx \int_0^{\infty} \left[\vec{\nabla}_{x,y} n(x_1, y_1, z) \cdot (\vec{r}_2 - \vec{r}_1) \right] \frac{dz}{\mu}$$

- *The interferometer is sensitive to the gradient of the TEC*



Total Electron Content Sensitivity (2 of 2)

- For ionospheric physics purposes, interferometer *sensitivity to phase changes* and *insensitivity to absolute phase* implies that:
 - *Interferometers are insensitive to laminar ionospheres*
 - *Determination of “large scale” phase screens is an under-determined problem*
 - Constant TEC terms are lost
 - *Also, ionospheric tomography using interferometers is under-determined – due to absolute phase insensitivity and due to insufficient vertical resolution*
 - Similar to Computerized Ionospheric Tomography which measures TEC relative to some position (usually the point of closest approach)
 - But instead of a few bias terms ~ number of stations – tomography would require thousands of bias terms ~ number of sources the number of stations!
- But interferometers are very sensitive to TEC changes to ~0.001 TECU/deg phase (at ~80 MHz)
 - *Great for measuring and monitoring gradients and their time variation*
 - *Great for detecting traveling structures*
 - *Maybe use frequency dependence to provide additional information?*

